Corrosion Inhibition, Adsorption and Thermodynamic Properties of Poly (Sodium 4-Styrenesulfonate) on Carbon Steel in Phosphoric Acid Medium.

Attar Tarik[a,b*], Abbes Benchadli[a], Messaoudi Boulanouar[a,b], Esma Choukchou-Braham[a]

[a]*Laboratory of ToxicoMed, University of Abou Bekr Belkaïd, B.P.119, Tlemcen, 13000, Algeria*

[b]*Higher School of Applied Sciences, P.O. Box 165 RP, Tlemcen, 13000, Algeria*

att.tarik@gmail.com, t.attar@essa-tlemcen.dz

Keywords: *Poly (sodium 4-styrenesulfonate), Adsorption mechanism, thermodynamic parameters, SEM, DFT.*

The use of polymers as corrosion inhibitors has attracted much attention due to their low prices, inherent stability, availability and cost-effectiveness. The corrosion inhibiting effect of poly(sodium-4-styrenesulfonate) on carbon steel in phosphoric acid solution has been investigated using weight loss and scanning electron microscopy techniques (SEM) and theoretical calculations based on density functional theory (DFT). In the presence of 1.0×10^{-3} mol/L of inhibitor, a maximum inhibition effect of 98.06 % was observed. The influence of the concentration of the inhibitor, the temperature of the solution and the immersion time on the corrosion of carbon steel was investigated. Activation parameters such as activation energy (E_{act}), activation enthalpy (ΔH_{act}), activation entropy (ΔS_{act}), heat of adsorption (Q_{ads}) and adsorption free energy (ΔG_{ads}) were evaluated based on the effect of temperature on the corrosion and inhibition processes. It was found that the adsorption behaviour of poly(sodium-4-styrenesulfonate) (PSS) follows the Langmuir isotherm and the free energy change values indicate mixed chemical and physical adsorption on the carbon steel surface. The results obtained with the different methods agree well.

Introduction

Carbon steel is used in various industries due to its cost effectiveness and high mechanical strength [1-2]. It is highly susceptible to corrosion when exposed to oxygen under extreme service conditions such as chemical contamination and moisture. This phenomenon of degradation causes enormous safety and economic losses in the form of lost production, replacement of corroded parts, accidents and public risks, especially in industry [3]. Various efforts have been made in the past to reduce the unfavourable reactions, mainly by common industrial developments such as acid pickling, acid descaling and acid cleaning, and the use of corrosion inhibitors is one of the best methods. Phosphoric acid is used in various industries such as chemical and electrolytic

polishing and oxide layer removal. On the other hand, phosphoric acid is known to be highly corrosive to ferrous materials, so it is necessary to limit or protect the attack on metallic materials. The effectiveness of inhibition depends on several variables, such as the chemical structure of the inhibitor and its quantity in the medium, the composition and type of metal, the aggressive electrolyte, the temperature and the immersion time. In addition, it also depends on the number of active adsorption centres in the molecule, its adsorption capacity and its electronic structure. Organic compounds containing polar functional groups with nitrogen, oxygen and/or sulphur in conjugated systems are generally used as corrosion inhibitors to reduce the corrosion rate of metals in acidic media [4-6]. Corrosion inhibition of these organic compounds is mainly observed by physical or chemical adsorption, which results from the interaction of the polar centres of the inhibitor with active sites on the metal surface [7-9]. Polymeric corrosion inhibitors have recently become widely used for the following reasons: They are considered environmentally friendly organic compounds, they are available, inexpensive and stable on the surfaces of metallic materials in corrosive environments, and they have multiple adsorption sites due to cross-functional groups. Previous work in the literature has reported some polymers that can be used as corrosion inhibitors for carbon steel in corrosive media [10-19]. Polymers such as gum tragacanth [10], polyaspartic acid [11], diamine-aromatic epoxy prepolymers [12], soy polymer and polyvinylpyrrolidone [13, 14], povidone-iodine [15], pentaglycidyl ether pentabisphenol A of phosphorus [16], sodium polyacrylates [17], gelatinous protein [18], maltodextrin and chitosan [19]. As an extension of the studies conducted on the use of polymers as corrosion inhibitors for carbon steel in acidic medium, we have investigated the use of poly(sodium-4-styrenesulfonate) as a corrosion inhibitor for carbon steel in phosphoric acid using various techniques; weight loss, (WL) scanning electron microscopy (SEM) and density functional theory (DFT).

Experimental

Materials and methods

The composition of carbon steel used in this work was (in % by weight): C: 0.37 %, Mn: 0.68 %, Cu: 0.16 %, Cr: 0.077 %, Ni: 0.059 %, Si: 0.023 %, S: 0.016 %, Ti: 0.011 %, Co: 0.009 % and the remaining part was Fe. The solution of 0.33 M phosphoric acid was prepared by diluting H_3PO_4 (85 %, Sigma-Aldrich) with double distilled water. Poly (sodium 4-styrenesulfonate) was prepared with (Mw ~70,000, powder, Sigma Aldrich). Five different concentrations 5.0×10^{-5}, 7.5×10^{-5}, 1.0×10^{-4}, 1.0×10^{-3} and 5.0×10^{-3} mol/L of PSS were prepared in 0.33 mol/L concentration of phosphoric acid.

Weight loss method

Weight loss measurement is a non-electrochemical technique used to determine corrosion rates and inhibitor effectiveness. It provides more reliable results than electrochemical techniques because the experimental conditions are more realistic. The weight loss method was carried out at 20 °C to 60 °C for 2 hours in 1.0 N phosphoric acid and the concentrations of inhibitor used ranged from 5.0×10^{-5} to 5.0×10^{-3} mol/L. In addition, the carbon steel samples were sanded with emery paper, washed with double distilled water, degreased with acetone and dried at room temperature. After the tests, the steel samples were washed again with double distilled water, dried and then weighed. All measurements were carried out in triplicate and the average value of the weight loss was noted. The corrosion rate (CR), inhibition efficiency (IE, %) and surface coverage (θ) of the carbon steel were determined both in the absence and presence of the inhibitor at different concentrations using equations (1), (2) and (3) [20, 21]:

$$CR = (W_1 - W_2) / (S \times t) \quad (1)$$

$$IE = 100 \times (CR - CR_{Inh}) / CR \quad (2)$$

$$\theta = IE / 100 \quad (3)$$

where CR and CR_{Inh} are the corrosion rates in the absence and presence of the inhibitor, respectively, and W_1 and W_2 are the weight losses of the carbon steel in the absence and presence of the inhibitors, respectively.

DFT Calculations

In this work, the quantum chemical calculations were performed using the Gaussian 09 W program suite. Density functional theory (DFT) is an application integrated in the commercial software (Gaussian). This application allowed the optimization of the geometry of single molecules at the B3LYP level with the basis set 6-31G(d). B3LYP with the Becke Lee-Yang-Parr three-parameter hybrid functional indeed gives good results, allowing to describe the behavior of organic compounds with high precision [22, 23]. The higher E_{HOMO} value expresses the tendency of the molecule to donate electrons, while the lower E_{LUMO} value indicates the ability of the molecule to accept electrons. The energy gap is then calculated as the difference between the E_{LUMO} and E_{HOMO} energies [24]:

$$\Delta E_{gap} = E_{LUMO} - E_{HOMO} \quad (4)$$

Low energy gap values indicate good reactivity for chemical interactions and good inhibitory activity. However, larger values of ΔE_{gap} indicate low reactivity for chemical interaction and low inhibitory effect. According to Koopman theorem [25], the negative value of E_{HOMO} is defined as ionization potential (I) and is given by:

$$I = -E_{HOMO} \quad (5)$$

The lowest unoccupied molecular orbital energy E_{LUMO} is another parameter whose negative value is defined as the electronic

affinity (A) according to the following expression [25]:

$$A = -E_{LUMO} \quad (6)$$

The hardness (η) of an atom or molecule is the energy required for its dismutation; it is the resistance to charge transfer. On the other hand, softness (S) reflects the ability of an atom or molecule to retain an acquired charge [2, 26] They can be represented as a function of ionization potential (I) and electron affinity (A) [27]:

$$\eta = (I - A)/2 = (E_{LUMO} - E_{HOMO})/2 \quad (7)$$

$$S = 2/(I - A) = 2/(E_{LUMO} - E_{HOMO}) \quad (8)$$

The global electrophilicity index (ω) is a measure of the energy decrease due to the maximum electron flow between donor and acceptor. It provides information about the nucleophilicity and electrophilicity of the inhibitory molecule. The electrophilicity index (ω) is calculated as follows [28]:

$$\omega = \mu^2 / 2\eta \quad (9)$$

The fraction of electrons transferred (ΔN) from the inhibitor molecule to the metal was calculated according to Pearson's electronegativity relationship [29]:

$$\Delta N = (\chi_{Fe} - \chi_{Inh})/2 \times (\eta_{Fe} + \eta_{Inh}) \quad (10)$$

where χ_{Fe} and η_{Fe}, χ_{inh} and η_{inh} denote the electronegativity and hardness of iron and inhibitor molecule, respectively. In this study, we used the theoretical value χ_{Fe} = 7.0 and η_{Fe} = 0 eV/mol for a metallic charge (I = A) because they are softer than the neutral metal atoms [30]. In a simple model of charge transfer for the donation and backdonation of charges, an electronic backdonation process can occur as a result of the interaction between the inhibiting molecule and the surface of a metal. The value of charge backdonation was calculated using the following expression [31]:

$$\Delta E_{back-donation} = -\eta/4 \quad (11)$$

The charges transferred to the molecule, are energetically favored when $\eta > 0$ and $\Delta E_{back\text{-}donation} < 0$.

Results and discussion

Effect of Acid Medium

Acid solutions are widely used in industry for removing mill scale from metal surfaces, acid pickling, acid descaling, acidifying oil wells and industrial acid cleaning. The inhibition effect of PSS is mainly used in various acidic media such as nitric acid, phosphoric acid, sulphuric acid, hydrochloric acid and perchloric acid. From **Figure 1**, the best inhibition efficiency (98.06%) is obtained in phosphoric acid solution compared to perchloric acid (44.35%), nitric acid (30.42%), chloric acid (15.45%) and sulphuric acid (11.66%). This could be due to the favourable adsorption of phosphate ions on the surface of carbon steel. The inhibitor molecules interact strongly with the metal surface in the presence of phosphate ions, which are normally characterised by a low adsorption capacity. On the other hand, the ions of perchlorate, nitrate, chloride and sulphate coordinate with the metal

surface and weaken it in adsorbing the inhibitor molecules. Moreover, the change in the effectiveness of inhibition compared to the change in the corrosive medium shows that the effectiveness of inhibition also depends on the type of corrosive medium. In this work, the study was conducted only in phosphoric acid, as PSS adsorbs better in this acid than in other acids tested.

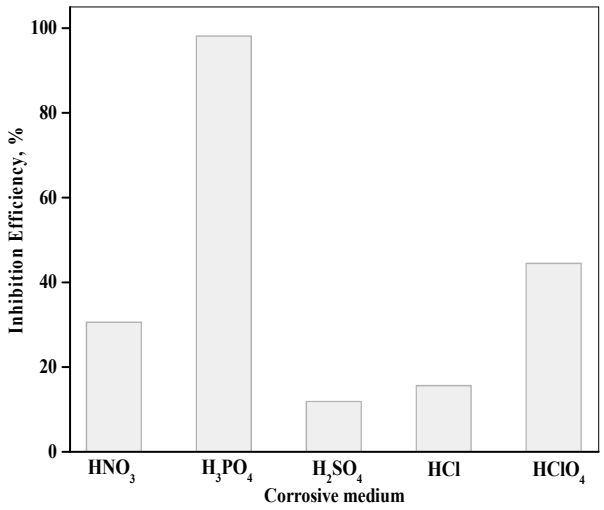

Figure 1. Variation of inhibition efficiency with different acid medium for carbon steel (PSS 1.0×10^{-3} mol/L for 2 h and at 303 K).

Effect of concentration

The anticorrosive performance of PSS against corrosion was investigated by monitoring the weight loss during the process. The weight loss was determined in phosphoric acid in the absence and presence of different concentrations of the inhibitor during a two-hour immersion period. From **Table 1** the inhibitory effect of PSS increased to 99 % at a concentration of 1.0×10^{-3} mol/L. The inhibitory effect increases with the increase in the concentration of inhibitor. PSS was found to cover the surface of carbon steel well. At the lowest concentration of PSS (5.0×10^{-5} mol/L), the surface coverage (θ) on the carbon steel is significant 0.84.

Table 1. The values of corrosion rate, inhibition efficiency and surface coverage by weight loss for different concentrations of PSS in H_3PO_4 at different temperatures.

C_{inh}, mol/L	T, K	CR, mg/cm² h	IE, %	Θ
0.0	293	0.10366	-	-
	303	0.18660	-	-
	313	0.33589	-	-
	323	0.60460	-	-
	333	1.08828	-	-
5.0×10^{-5}	293	0.01624	84.33	0.843
	303	0.03876	79.23	0.792
	313	0.10040	70.11	0.701
	323	0.24698	59.15	0.591
	333	0.63196	41.93	0.419
7.5×10^{-5}	293	0.01077	89.61	0.896
	303	0.03002	83.91	0.839
	313	0.07554	77.51	0.775
	323	0.24009	60.29	0.602
	333	0.54316	50.09	0.501
1.0×10^{-4}	293	0.00514	95.04	0.950
	303	0.01726	90.75	0.907
	313	0.06157	81.67	0.81
	323	0.18029	70.18	0.701
	333	0.43891	59.67	0.596
1.0×10^{-3}	293	0.00103	99.01	0.990
	303	0.00362	98,06	0.980
	313	0.02761	91.78	0.917
	323	0.13108	78.32	0.783
	333	0.12769	65.41	0.654
5.0×10^{-3}	293	0.00081	99.22	0.992
	303	0.00261	98,60	0.986
	313	0.02674	92.04	0.920
	323	0.37644	78.88	0.788
	333	0.36925	66.07	0.660

According to **Table 1**, this result confirms that an inhibitor added to a corrosive medium in a small amount regulates the rate of metal dissolution by forming a preventive barrier film, which in turn halts the progression of the corrosive reaction [3, 32]. At higher temperatures, the PSS was desorbed from the surface of the carbon steel. It was also observed that as the temperature increased, the corrosion rate (CR) also increased. This inhibitor was found to work well at lower temperatures and inhibit poorly at higher temperatures.

Effect of immersion time

The results presented in **Figure 2** show the effect of immersion time on the inhibition effect and the change in weight loss of carbon steel immersed in 0.33 M H_3PO_4 solution at 303 K in the absence and presence of PSS at different time intervals up to 24 hours. We see that the two curves are almost linear with and without inhibitor; this means that the metal surface is free from insoluble corrosion products. This means that the metal surface is free of insoluble corrosion products. From this we can conclude that this amount is almost constant from the first hour of immersion, which leads us to the conclusion that the immersion time has no significant effect on the corrosion inhibition of carbon steel in phosphoric acid by PSS. The maximum corrosion IE of 98.06% is reached after 2 hours of immersion (**Figure 2**). The decrease in inhibition effect was attributed to the desorption of the corrosion inhibitors from the surface of the carbon steel. It is evident that once the inhibitor molecules were desorbed from the metal surface, they became inactive and therefore were no longer involved in the inhibition process.

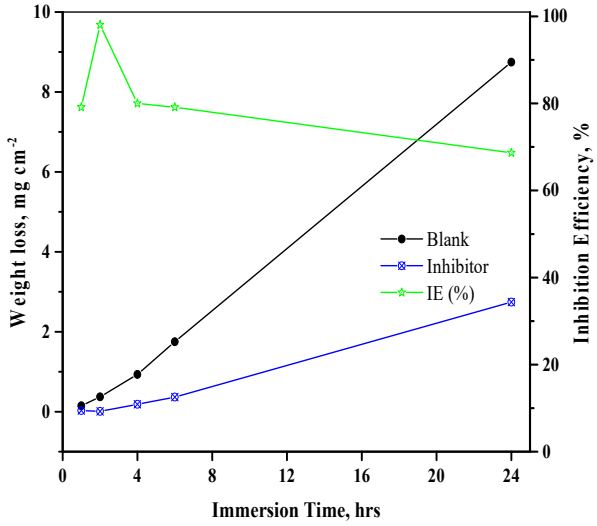

Figure 2. Variation of weight loss and inhibition efficiency vs immersion time for carbon steel at 1.0×10^{-3} mol/L of PSS.

Adsorption Mechanisms

In general, the adsorption of the inhibitor on the metal surface is the most important step in the inhibition mechanism, and the adsorption isotherm is a suitable method for characterising the inhibitor/metal/environment system. Different models of adsorption isotherms can be used to explain the adsorption process. A better agreement of the weight loss data was obtained by the Langmuir isotherm defined by equation (12) [33]:

$$C_{Inh} / \theta = 1 / K_{ads} + C_{Inh} \qquad (12)$$

where C_{Inh} is the inhibitor concentration, θ is the degree of coverage on the metal surface, and K_{ads} is the equilibrium constant for the

adsorption-desorption process calculated by the reciprocal of the intercept of the isotherm line at different temperatures (**Table 2**). The free energy of adsorption (ΔG_{ads}) on the carbon steel surface can be calculated by the following equation (13) [34]:

$$\Delta G_{ads} = RT \times \ln(55.5 \times K_{ads}) \quad (13)$$

where R is the gas constant (J/mol K) and T is the absolute temperature (K). The constant value of 55.5 is the concentration of water in the solution (mol/L).

Analysis of the variation of $C_{inh:}/\theta$ ratio as a function of C_{inh} is linear (the regression coefficients are all equal to 1.0 see **Table 2**).

Table 2. The thermodynamic parameters of adsorption of PSS in phosphoric acid on the carbon steel surface at different temperatures.

T, K	R^2	K_{ads}, m^3/mol	ΔS_{ads}, J/mol K	ΔG_{ads}, kJ/mol
293	1	73.757	-10.39	-37.08
303	1	48.814	-29.80	-37.31
313	1	33.095	-64.95	-37.53
323	1	154.617	-152.31	-42.87
333	1	92.049	-178.77	-42.76

This shows that the adsorption of PSS on the carbon steel surface in phosphorus-containing medium obeys the Langmuir adsorption isotherm. The values of the heat of adsorption were determined using the kinetic thermodynamic model [35].

$$\theta/(1-\theta) = qC_{Inh} \times \exp(-Q_{ads}/RT) \quad (14)$$

where q is a constant, C_{Inh} is the inhibitor concentration, θ is the occupied site, and (1-θ) is the unoccupied site not occupied by the inhibitor. **Figure 3** shows the curves of ln(θ/1-θ) versus 1/T for all PSS concentrations. The obtained lines show a slope equal to (Q_{ads}/R). The negative values of Q_{ads} (**Table 3**) indicate that the adsorption on the carbon steel surface is exothermic. The higher values of the equilibrium constant of adsorption are good indicators of strong adsorption of the studied inhibitors on the carbon steel surface.

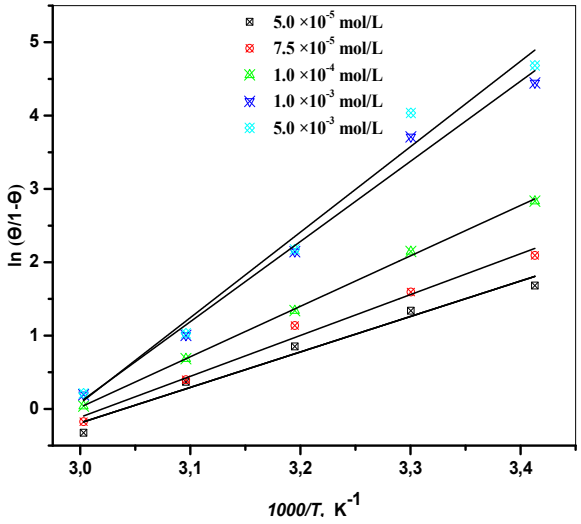

Figure 3. Application of kinetic–thermodynamic model on PSS inhibitor of carbon steel surface in phosphoric acid.

Table 3. Calculated values of heat of adsorption (Q_{ads}) for carbon steel in H_3PO_4.

C_{Inh}, mol/L	R^2	Q_{ads}, kJ/mol
5.0×10^{-5}	0.975	-40.23
7.5×10^{-5}	0.986	-46.34
1.0×10^{-4}	0.999	-57.21
1.0×10^{-3}	0.986	-89.02
5.0×10^{-3}	0.981	-96.93

The negative value of the adsorption entropy shows that the destruction on the metal surface was reduced and the positive value shows that the disorder of the system increased [2]. The distinction between chemisorption and physisorption depends on the estimated value of ΔG_{ads}. When the values of adsorption free

energy are more than -20 kJ/mol, the physisorption mechanism is generally preferred, while for values of ΔG_{ads} of -40 kJ/mol or less, the adsorption process is chemisorption. In this study, the mean value of ΔG_{ads} of -39.50 kJ/mol is almost slightly less negative than -40 kJ/mol, indicating that the adsorption of inhibitor molecules is not only physisorption or chemisorption, but obeys a comprehensive adsorption (physical and chemical adsorption). A limited increase in the absolute value of ΔG_{ads} was observed with an increase in temperatures, indicating that adsorption was slightly more favourable with increasing experimental temperature, suggesting that chemisorption is the major contributor, while the contribution of physisorption to the adsorption mechanism is minor. The absolute value of Q_{ads} for the physisorption process is less than 40 kJ/mol, while the value for the chemisorption process approaches 100 kJ/mol [36]. In the present work, the Q_{ads} values are larger than the physisorption heat of adsorption, but smaller than the chemisorption heat of adsorption, once again emphasising that both physisorption and chemisorption take place. Since adsorption is an exothermic process, according to thermodynamic principles it must be accompanied by a decrease in entropy. During the inhibition process, the molecules of the inhibitor in solution become protonated and positively charged, as does the metal surface in acidic media. Phosphate ions are selectively adsorbed onto the metal, creating an excess of negative charge on the metal surface. This promotes the adsorption of protonated PSS on the surface by electrostatic attraction, thus reducing the dissolution of iron (physical adsorption). Furthermore, the inhibitors on the carbon steel surface were chemically adsorbed by donor/acceptor interactions between free electron pairs of the heteroatoms and the free d-orbital of the iron atoms of the surface metal. This type of electron transfer leads to an excessive accumulation of negative charge on the electron-rich metallic surface, causing it to transfer its electrons to the vacant π^* molecule orbitals of the inhibitors by retrodonation. In summary, the adsorption of this inhibitor on the carbon steel surface is extensive and involves both physisorption and chemisorption.

Activation Parameters

The inhibitory mechanism can be understood in terms of the thermodynamic and activating parameters. The Arrhenius equation can be successfully used to show the influence of temperature on the inhibitory effect of the inhibitor under study. It is represented by the following equation [15]:

$$CR = A \times \exp(-\Delta E_{act} / RT) \qquad (15)$$

where CR is the corrosion rate of carbon steel, A is the Arrhenius pre-exponential factor, E_{act} (kJ/mol) is the activation energy, R is the gas constant (8.314 J/mol K) and T is the temperature (K).

The values of apparent activation energy (E_{act}) for carbon steel in phosphoric acid in presence and absence of different concentrations of PSS were obtained from the slope of ln(CR) versus 1/T. The values of activation enthalpy (ΔH_{act}) and activation entropy (ΔS_{act}) can be calculated by the slope ($-\Delta H_{act}/R$) and intercept ($\ln(R/Nh)+\Delta S_{act}/R$) of ln(CR/T) versus 1/T , using the following transition state equation (16) [15]:

$$\ln(CR/T)=\left[(\Delta S_{act}/R)+\ln(R/Nh)\right]-\Delta H_{act}/RT \quad (16)$$

where h is Planks constant, N is Avogadro's number, ΔS_{act} is the entropy of activation, and ΔH_{act} is the enthalpy of activation.

All the activation kinetic parameters (E_{act}, ΔH_{act}, ΔS_{act} and ΔG_{act}) are estimated and listed in Table 4. The lower or unchanged values of E_{act} for the inhibited systems compared to the blank test indicate a chemisorption mechanism, while the higher values of E_{act} in the presence of PSS are indicative of a physical adsorption mechanism. From **Table 4**, the E_{act} values increase with increasing concentration of inhibitor, indicating that the adsorption surface area increases with increasing concentration of inhibitor due to easier adsorption. The positive values of ΔH_{act} indicate that the formation of the activated complex is an endothermic process [37]. The average value of the difference between activation energy and enthalpy change (E_{act}-ΔH_{act}) is 2.59 kJ/mol for all PSS concentrations, which is the exact value of the product of the gas constant and the average temperature of the experiment (313 K). This result shows that the corrosion process is a unimolecular reaction with the evolution of hydrogen gas [32].

Table 4. Activation parameters of carbon steel corrosion in the presence of PSS in H_3PO_4.

C_{inh}, mol/L	R^2_{eq15}	E_{act}, kJ/mol	R^2_{eq16}	ΔH_{act}, kJ/mol	ΔS_{act}, J/mol K	$\Delta G_{act\ (313K)}$, kJ/mol
Blank	0.998	47.64	0.998	45.05	-110.07	79.50
5.0×10^{-5}	0.997	74.33	0.997	71.74	-34.75	82.61
7.5×10^{-5}	0.997	80.45	0.997	77.85	-17.04	83.18
1.0×10^{-4}	0.998	91.31	0.998	88.72	14.46	84.19
1.0×10^{-3}	0.989	125.03	0.991	122.43	114.98	86.44
5.0×10^{-3}	0.982	131.03	0.986	128.44	133.10	86.77

In the presence of the inhibitor (**Table 4**), the value of ΔS_{act} increases. This is mainly explained by an increase in disorder as the reactants are converted into activated complexes. The shift to a positive value of ΔS_{act} (from 1×10^{-4} mol/L) means that the activated complex in the rate-determining step is dissociation rather than association, implying that disorder increases from the reactants to the activated complex [2]. The free energy of

activation values was positive with increasing concentration. These values of ΔG_{act} are due to the formation of unstable activated complex in the rate determining transition state.

Quantum chemical calculation

Computational methods have a potential application towards the design and development of organic corrosion inhibitors in the corrosion field. The electronic structure of the PSS was elucidated using the B3LYP/6-31G* level of theory. The highest occupied molecular orbital (HOMO), molecular structure and lowest unoccupied molecular orbital (LUMO) studied for PSS are shown in **Figure 4**.

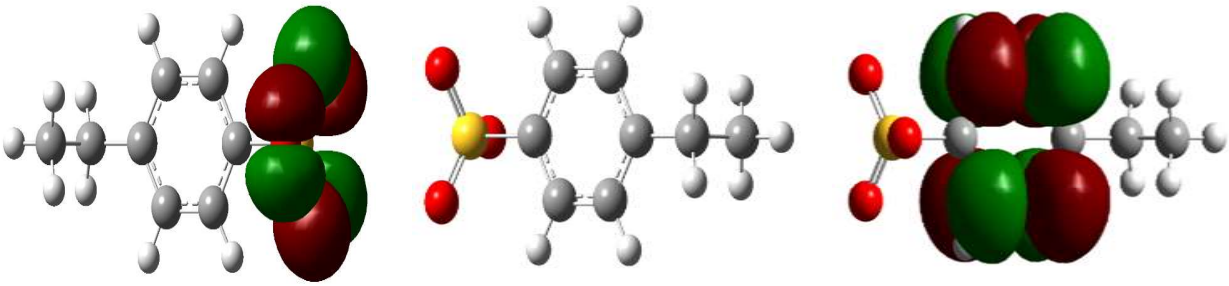

Figure 4. The frontier molecular orbital density distributions of PSS: HOMO (left); LUMO (right) and optimised structure (centre).

The E_{HOMO} and E_{LUMO} values, global hardness (η), electrophilicity index (ω), softness (S), gap energy (ΔE_{gap}), number of electrons transferred (ΔN) and back-donation of charges ($\Delta E_{back\text{-}donation}$) were calculated and listed in **Table 5**. Increasing E_{HOMO} values facilitate adsorption and thus inhibition by influencing the transport process through the adsorbed layer on the steel surface [38]. The E_{LUMO} value indicates the ability of the molecule to accept electrons. The lower the E_{LUMO} value, the more likely it is that a molecule can accept electrons. Thus, a higher hardness value (2.41 eV) is an indication of higher stability and lower reactivity. In addition, the best inhibitor is the one with the highest value of softness (S), which also indicates that a higher number of electrons are transferred. A high value of electrophilicity (ω) characterises a good electrophile, while a small value of electrophilicity describes a good nucleophile; this index is useful to predict the direction of corrosion. The values of the ΔE_{gap} (4.82 eV) are important; lower values of the energy difference lead to a higher inhibition effect because the excitation energy required to remove an electron from the last occupied orbital is low. When the fraction of transferred electrons (ΔN) is less than 3.6 eV, the inhibition effect increases with increasing electron donor capability at the metal surface. The value of ΔN determined for the PSS molecule is 1.61 eV, indicating that this inhibitor is an electron donor, while the carbon steel surface is the acceptor. The $\Delta E_{backdonation} < 0$ and $\eta > 0$ indicate that the backdonation of the molecule is energetically favoured [2].

Table 5. HOMO and LUMO energies, global reactivity indices η, ω, S, ΔE_{gap}, ΔN and $\Delta E_{back\text{-}donation}$, for the PSS studied compound at B3LYP/6-31G* level of theory.

Substrate	E_{HOMO}, eV	E_{LUMO}, eV	η, eV	ω, eV	S, eV^{-1}	ΔE_{gap}, eV	ΔN, eV	$\Delta E_{back\text{-}donation}$, eV
PSS	-1.65	3.17	2.41	0.12	0.41	4.82	1.61	-0.62

Surface analysis

Scanning electron microscopy (SEM) was carried out to investigate the effects of poly(sodium-4-styrene sulfonate) on the morphology of the steel surface. The SEM observations (**Figure 5**) of the carbon steel substrate surfaces were carried out at the same magnification (×1000) to see the progress that occurred during the corrosion process in the presence and absence of the inhibitor studied in 0.33 M H_3PO_4 electrolyte. The carbon steel shows considerable surface damage in the absence of the inhibitor due to the aggressive acid attack. However, in the presence of PSS, the surface damage is much less. This improvement can be attributed to the adsorption of PSS on the metal surface and the formation of a protective film that isolates the surface of the carbon steel from the corrosive acidic environment [15, 39].

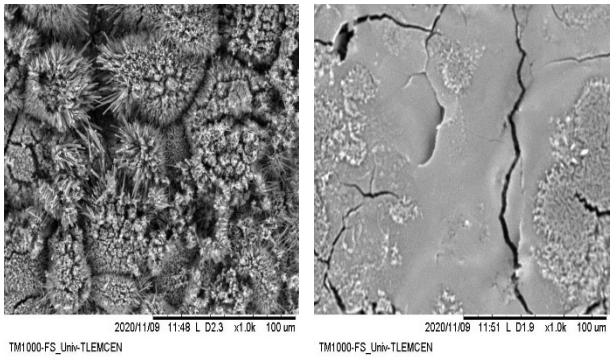

Figure 5. SEM Images of the surface of carbon steel in H_3PO_4 in the absence (left) and in the presence (right) of 1.0×10^{-3} mol/L poly(sodium 4-styrenesulfonate)

Conclusions

The results obtained show that poly(sodium-4-styrenesulfonate) acts as an excellent effective inhibitor for the corrosion of carbon steel in 1 N phosphoric acid solution. The results show that PSS is effective in the order of phosphoric acid - hydrochloric acid > nitric acid - hydrochloric acid > sulphuric acid. PSS acted as a good corrosion inhibitor for carbon steel in H_3PO_4 and showed maximum efficiencies of 99.22% and 84.33% at low concentration of inhibitor. The adsorption of poly(sodium-4-styrenesulfonate) on the surface of carbon steel follows the Langmuir adsorption isotherm. The values of the thermodynamic parameters show that the adsorption process is both physical and chemical. The result found with the PSS weight loss method was confirmed by both quantum chemical calculations and scanning electron microscopy.

Acknowledgements

The authors would like to thank the Ministry of Higher Education and Scientific Research of Algerian Government and the Higher School of Applied Sciences for their fruitful support.

References

[1] Abeng FE, Ikpi ME, Anadebe VC, Emori W. Metolazone compound as corrosion inhibitor for API 5L X-52 steel in hydrochloric acid solution. Bulletin of the Chemical Society of Ethiopia 2020;34(2):407-418.

[2] Attar T, Benchadli A, Messaoudi B, Benhadria N, Choukchou-Braham E. Experimental and Theoretical Studies of Eosin Y Dye as Corrosion Inhibitors for Carbon Steel in Perchloric Acid Solution. Bulletin of Chemical Reaction Engineering & Catalysis 2020;15(2):454-464.

[3] Attar T, Nouali F, Kibou Z, Benchadli A, Messaoudi B, Choukchou-Braham E, Choukchou-Braham N. Corrosion inhibition, adsorption and thermodynamic properties of 2-aminopyridine derivatives on the corrosion of carbon steel in sulfuric acid solution. Journal of Chemical Sciences 2021;133(4):109.

[4] Dhaundiyal P, Bashir S, Sharma V, Kumar A. An investigation on mitigation of corrosion of mildsteel by Origanum vulgare in acidic medium. Bulletin of the Chemical Society of Ethiopia 2019;33(1):159-168.

[5] Mourya P, Singh P, Tewari A, Rastogi R, Singh M. Relationship between structure and inhibition behaviour of quinolinium salts for mild steel corrosion: Experimental and theoretical approach. Corrosion Science 2015;95:71-87.

[6] Attar T, Benchadli A, Mellal T, Dali-Youcef B, Choukchou-Braham E. Use of Experimental Designs to Evaluate the Influence of Methyl Green Dye as a Corrosion Inhibitor for Carbon Steel in Perchloric Acid. Malaysian Journal of Chemistry 2021;23(1):60-69.

[7] Popova A, Christov M, Vasilev A. Mono- and dicationic benzothiazolic quaternary ammonium bromides as mild steel corrosion inhibitors. Part III: Influence of the temperature on the inhibition process. Corrosion Science 2015;94:70-78.

[8] Ostapenko G, Gloukhov P, Bunev A. Investigation of 2-cyclohexenylcyclohexanone as steel corrosion inhibitor and surfactant in hydrochloric acid. Corrosion Science 2014;82:265-270.

[9] Özcan M, Toffoli D, Üstünel H, Dehri T. Insights into surface-adsorbate interactions in corrosion inhibition processes at the molecular level. Corrosion Science 2014;80:482-486.

[10] Mobin M, Rizvi M, Olasunkanmi L, Ebenso E. Biopolymer from Tragacanth Gum as a Green Corrosion Inhibitor for Carbon Steel in 1 M HCl Solution. ACS Omega 2017;2(7):3997-4008.

[11] Chen T, Zeng D, Zhou S. Study of Polyaspartic Acid and Chitosan Complex Corrosion Inhibition and Mechanisms. Polish Journal of Environmental Studies 2018;27(4):1441-1448.

[12] Dagdag O, Safi Z, Hsissou R, Erramli H, El Bouchti M, Wazzan N, Guo L, Verma C, Ebenso E, El Harfi A. Epoxy pre-polymers as new and effective materials for corrosion inhibition of carbon steel in acidic medium: Computational and experimental studies. Scientific Reports 2019;9(1):1-14.

[13] Valbon A, Neves M, Echevarria A. Anticorrosive Effect of PVP 40000 Against AISI 1020 Carbon Steel in HCl. Materials Research 2018;21(6):1-7.

[14] Benchadli A, Attar T, Messaoudi B, Choukchou-Braham E. Polyvinylpyrrolidone as a Corrosion Inhibitor for Carbon Steel in a Perchloric Acid Solution: Effect of Structural Size. Hungarian Journal of Industry and Chemistry 2021;49(1):59-69.

[15] Benchadli A, Attar T, Choukchou-Braham E. Inhibition of Carbon Steel Corrosion in Perchloric Acid Solution by Povidone Iodine. Physical Chemistry Research 2019;7(4):837-848.

[16] Hsissou R, Abbout S, Seghiri R, Rehioui M, Berisha A, Erramli H, Assouag M, Elharfi A. Evaluation of corrosion inhibition performance of phosphorus polymer for carbon steel in [1 M] HCl: Computational studies (DFT, MC and MD simulations). Journal of Materials Research and Technology 2020;9(3):2691-2703.

[17] Branzoi F, Băran A, Ludmila A, Alexandrescu E. The inhibition action of some organic polymers on the

corrosion carbon steel in acidic media. Chemical Papers 2020;74(12):4315-4335.

[18] Farag A, Ismail A, Migahed M. Squid By-product Gelatin Polymer as an Eco-friendly Corrosion Inhibitor for Carbon Steel in 0.5 M H2SO4 Solution: Experimental, Theoretical, and Monte Carlo Simulation Studies. Journal of Bio- and Tribo-Corrosion 2019;6(1):16.

[19] Abdallah M. Maltodextrin and Chitosan Polymers as Inhibitors for the Corrosion of Carbon Steel in 1.0 M Hydrochloric Acid. International Journal of Electrochemical Science 2020;15:5650-5663.

[20] Attar T, Benchadli A, Choukchou-Braham E. Corrosion inhibition of carbon steel in perchloric acid by potassium iodide. International Journal of Advanced Chemistry 2019;7(1):35-41.

[21] Benchadli A, Attar T, Choukchou-Braham E. Corrosion inhibition of carbon steel (XC 38) in hydrochloric acid by potassium iodide. Journal of Advanced Research in Science and Technology 2018;5(2):834-844.

[22] Tigori M, Kouyaté A, Kouakou V, Niamien P, Trokourey A. Inhibition Performance of Some Sulfonylurea on Copper Corrosion in Nitric Acid Solution Evaluated Theoretically by DFT Calculations. Open Journal of Physical Chemistry 2020;10(03):139-157.

[23] Chugh B, Singh A, Thakur S, Pani B, Lgaz H, Chung I, Jha R, Ebenso E. Comparative Investigation of Corrosion-Mitigating Behavior of Thiadiazole-Derived Bis-Schiff Bases for Mild Steel in Acid Medium: Experimental, Theoretical, and Surface Study. ACS Omega 2020;5(23):13503-13520.

[24] Benhadria N, Messaoudi B, Attar T. The Study of the Correlation between the Detection Limit and the Energy Stability of Two Antimony Complexes by Means of Conceptual DFT. Malaysian Journal of Chemistry 2020;22(2):111-120.

[25] Danaee I, Ramesh Kumar S, Rashvand Avei M, Vijayan M. Electrochemical and Quantum Chemical Studies on Corrosion Inhibition Performance of 2,2'-(2-Hydroxyethylimino)bis[N-(alphaalpha-dimethylphenethyl)-N-methylacetamide] on Mild Steel Corrosion in 1M HCl Solution. Materials Research 2020;23(2):1-16.

[26] Gad E, Azzam E, Halim S. Theoretical approach for the performance of 4-mercapto-1-alkylpyridin-1-ium bromide as corrosion inhibitors using DFT. Egyptian Journal of Petroleum 2018;27(4):695-699.

[27] Benhadria N, Attar T, Messaoudi B. Understanding the Link Between the Detection Limit and the Energy Stability of Two Quercetin–Antimony Complexes by Means of Conceptual DFT. South African Journal of Chemistry 2020;73(1):120–124.

[28] Attar T, Messaoudi B, Benhadria N. DFT Theoretical Study of Some Thiosemicarbazide Derivatives with Copper. Chemistry & Chemical Technology 2020;14(1):20-25.

[29] Musa A, Kadhum A, Mohamad A, Takriff M. Molecular dynamics and quantum chemical calculation studies on 4,4-dimethyl-3-thiosemicarbazide as corrosion inhibitor in 2.5M H2SO4. Materials Chemistry and Physics 2011;129(1-2):660-665.

[30] Alaoui K, El Kacimi Y, Galai M, Serrar H, Touir R, Kaya S, Kaya C, Ebn Touhami M. New triazepine carboxylate derivatives: correlation between corrosion inhibition property and chemical structure. International Journal of Industrial Chemistry 2020;11(1):23-42.

[31] Guo L, Safi Z, Kaya S, Shi W, Tüzün B, Altunay N, Kaya C. Anticorrosive Effects of Some Thiophene Derivatives Against the Corrosion of Iron: A Computational Study. Frontiers in Chemistry 2018;6:1-12.

[32] Attar T, Larabi L, Harek Y. Inhibition effect of potassium iodide on the corrosion of carbon steel (XC 38) in acidic medium. International Journal of Advanced Chemistry 2014;2(2):139-142.

[33] Okechukwu Dominic O, Valentine Chikaodili A, Chizoba Sandra O. Optimum prediction for inhibition efficiency of Sapium ellipticum leaf extract as corrosion inhibitor of aluminum alloy (AA3003) in hydrochloric

acid solution using electrochemical impedance spectroscopy and response surface methodology. Bulletin of the Chemical Society of Ethiopia 2020;34(1):175-191.

[34] Attar T, Larabi L, Harek Y. Corrosion inhibition of cold rolled steel in 0.5M H2SO4 by potassium iodide. Der Pharma Chemica 2014;6(4):181-186.

[35] El Faydy M, Lakhrissi B, Jama C, Zarrouk A, Olasunkanmi L, Ebenso E, Bentiss F. Electrochemical, surface and computational studies on the inhibition performance of some newly synthesized 8-hydroxyquinoline derivatives containing benzimidazole moiety against the corrosion of carbon steel in phosphoric acid environment. Journal of Materials Research and Technology 2020;9(1):727-748.

[36] Noor E, Al-Moubaraki A. Thermodynamic study of metal corrosion and inhibitor adsorption processes in mild steel/1-methyl-4[4′(-X)-styryl pyridinium iodides/hydrochloric acid systems. Materials Chemistry and Physics 2008;110(1):145-154.

[37] Attar T, Benchadli A, Choukchou-Braham E. Inhibition of corrosion of copper by polyvinylpyrrolidone-iodine in sulfuric acid medium. Algerian Journal of Materials Chemistry 2022;5(1):1-8.

[38] Sahrane M, Ghailane T, Galai M, Souizi A, Touhami M, Ghailane R, Touir R. Experimental and Theoretical Studies for Mild Steel Corrosion Inhibition in 1.0 M HCl by Two Stereoisomers of Benzothiazinone Derivatives. Portugaliae Electrochimica Acta 2020;38(1):1-17.

[39] Faiz M, Zahari A, Awang K, Hussin H. Corrosion inhibition on mild steel in 1 M HCl solution by Cryptocarya nigra extracts and three of its constituents (alkaloids). RSC Advances 2020;10(11):6547-6562.